JOURNAL OF MATERIALS SCIENCE 26 (1991) 1431–1442

Gas entrapment and evolution in prealloyed aluminium powders

J. L. ESTRADA, J. DUSZCZYK, B. M. KOREVAAR
Laboratory for Materials Science, Faculty of Chemical Technology and Materials Science, Delft University of Technology, Rotterdamseweg 137, 2628 AL Delft, The Netherlands

Part of a comprehensive research programme involving different aspects of degassing of powder metallurgy (P/M) aluminium alloys carried out in the P/M Group of the Delft University of Technology, is reported. The fundamental aspects of moisture and gas evolution during degassing of a porous billet are described in a semi-quantitative manner using a kinetic approach. During degassing of Al–20Si–X P/M alloys, at temperatures up to 550 °C, the partial pressures of moisture and hydrogen were within the range 10^{-4} to 10^{-7} mbar. The thermodynamics of gas desorption is mainly influenced by temperature which is the critical degassing parameter. It appears that the diffusion of aluminium through the oxide layer can explain, to a large extent, the kinetics of degassing of aluminium powders. A shift in the release of moisture and hydrogen towards higher temperatures is due to the presence of MgO in the surface layer, compared to the situation when only Al_2O_3 builds the oxide film. Thermodynamical data indicate that the reaction of magnesium with water vapour proceeds more intensely than that between aluminium and water vapour.

1. Introduction

In terms of industrial applications, high-strength Al–Si–X powder alloys form a rapidly expanding field where some important property improvements have been achieved. However, production processes and techniques can still be improved. In pursuit of these improvements, special attention has been focused on high silicon content powder metallurgy (P/M) aluminium alloys where the properties at high temperatures are an important goal [1–4]. In the application of these aluminium alloys to automotive parts, such as pistons, some properties have been well characterized but many details of the production process, which are still not very clear, require further investigation as in the case of surface reactions during the vacuum degassing of powders before consolidation.

An oxide layer is formed on the powder particle surface during the production, which is amorphous and initially ductile. This layer shows a strong tendency for hydration reactions when exposed to humid environments. Such hydration reactions lead to the presence of both chemically bonded (i.e. primarily as hydroxides $Al_2O_3 \cdot 3H_2O$, or oxy-hydroxides) and physically adsorbed water and oxygen at the powder particle surfaces.

The vacuum degassing, prior to consolidation by hot working, is an important step in the processing of P/M aluminium alloys because it removes moisture, adsorbed hydrogen and oxygen, decomposes hydrated oxides and supposedly transforms the ductile aluminium hydroxide into brittle crystalline γ-alumina [5]. With inadequate degassing the product can be porous and blistered, and the break-up of the surface oxide film is insufficient to give a good bonding of the particles during hot consolidation. Degassing also minimizes the possibility of additional oxidation of the powder during subsequent processing.

Although degassing, prior to consolidation and subsequent hot working, has been considered for many years as a fundamental step in the processing of P/M aluminium alloys, only over the last 5 years has a rapid development of this processing step taken place with the increased production of high-strength high-temperature aluminium alloys. The use of a degassing step, during the processing of alloys using ceramic particles and fibres as reinforcements, has been reported [6–12]. Practically all the results involving the degassing step, during the processing of P/M aluminium alloys, so far reported in the literature refer to the following systems: Al–Cr–X, Al–Cu–X, Al–Fe–X, Al–Li–X, Al–Mg–X, Al–Ni–X and Al–Zn–X. Only a few of them, including those written by the present authors [4, 13–16], concern the very important Al–Si–X system.

It must be noted that since the famous work about kinetics of degassing of aluminium powders published by the Soviet researchers Litvintsev and Arbuzova [17] in 1967, all of the work subsequently published has been essentially based on that paper. The majority of the reported results are based on a strict production engineering approach, without describing the fundamental aspects of degassing [18–67].

The work reported in this paper is a part of a comprehensive research programme involving different aspects of degassing of P/M aluminium alloys carried out in the P/M Group of the Delft University of

0022–2461/91 $03.00 + .12

Technology. The general approach of this research concerns surface properties of powders [68], conditions of gas entrapment during atomization and subsequent evolution during processing, the relationship between degassing conditions, subsequent processing and properties of the products.

Some fundamental aspects concerning gas entrapment and evolution, such as the relationship between surface composition and chemical reaction, are presented in this work. A semi-quantitative description of the process has been given using a thermodynamical and kinetical approach.

2. Theoretical background

Interactions of powdered metals with elements of the surrounding gas atmosphere are important processes in powder metallurgy. They are responsible for desired, as well as for undesired, changes of physical or mechanical properties of metallic powders. Hydrogen and oxygen and water vapour are of specific interest, because they can be present in condensed phases as components of compounds or as interstitially dissolved atoms, and in the gas phase as components of permanent gases. The pick-up of these gases has been recognized as a fundamental problem during atomization and subsequent post-atomization handling and storage of aluminium and its alloys [35, 36].

This environmental degradation of almost all P/M metals and P/M alloys in specific environments (both gaseous and liquid) with catastrophic brittle delayed failure at stresses, well below the normal engineering design values, has become an increasingly acute problem; a natural result as temperatures and pressures rise, alloy complexity increases, environments become more agressive, strength levels and applied stresses increase, and in general, demands on performance become more severe.

In order to understand the problem of gas entrapment in powders, a better knowledge of the production techniques and environmental contamination is essential, especially those techniques connected with gas atomization [68, 69], and the subsequent handling of the powders.

2.1. Powder production by atomization

Although this production technique has already been described in detail in previous papers [68, 69], it is necessary to extend this description in some aspects.

Atomization involves the formation of powder from molten metal using a spray of droplets. Both elemental and prealloyed powders can be formed by such processes. The flexibility of the approach, coupled with its applicability to different alloys and easy process control, make it an attractive alternative. A main feature of atomization is the general reliance on fusion-based technology. This reliance provides flexibility in both the feedstock, melt purification and alloy chemistry.

2.1.1. Gas atomization

Gas atomization is a two-fluid process involving the interaction of the liquid metal and the atomizing gas, which may be of sub- or supersonic velocity.

The metallic charge is melted either in an open furnace or in a vacuum induction melter and when the desired temperature of the molten bath is reached, the liquid is tapped into a tundish having a nozzle at its base. The melt must be superheated over the melting (liquidus) temperature. The liquid alloy flows through the nozzle as a continuous stream into the atomizing chamber below [70–72].

Atomization is produced by the kinetic energy of the atomizing fluid which most commonly is air, nitrogen, helium or argon [73]. The liquid-metal stream is disintegrated by rapid gas expansion out of a nozzle. The number and geometry of gas/metal configurations are unlimited; however, the main idea is to deliver energy (from a rapidly expanding gas) to the metal stream to form droplets. Fig. 1 [74] shows a typical schematic diagram of a vertical gas atomizer with a vacuum induction furnace, and Fig. 2 [70–72] shows representative gas-atomization configurations: (a) a two-jet configuration, and (b) an annular-ring configuration.

For reactive metals, a closed, inert gas-filled chamber is used to minimize oxidation. Gas atomization can be performed totally under inert conditions, thereby maintaining the integrity of high-alloy feedstock.

There are several interrelated processing and material variables involved in gas atomization, among them gas type, residual atmosphere, melt temperature and viscosity as it enters the nozzle, alloy type, metal feed rate, gas pressure, gas feed rate and velocity, nozzle geometry, and gas temperature. A big problem with gas atomization is the entrapment of gas in the powders. If the gas is insoluble (argon for example), the gas becomes part of the final product. The gas pores are sealed in hot extrusion but reform gas pockets on high-temperature re-exposure [73].

See and Johnston [75] have examined the breakup of the liquid-metal stream during gas atomization,

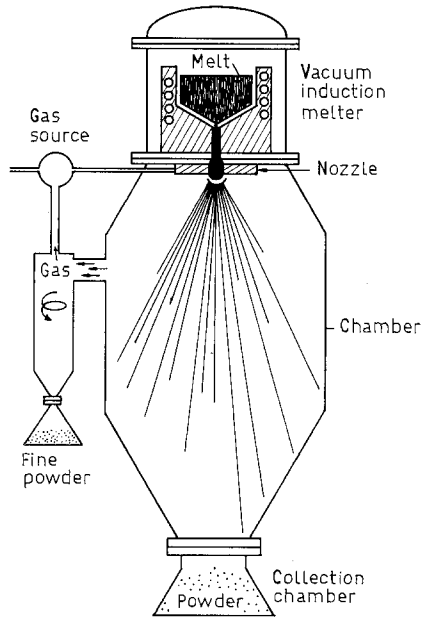

Figure 1 A vertical gas atomiser with a vacuum induction melter [74].

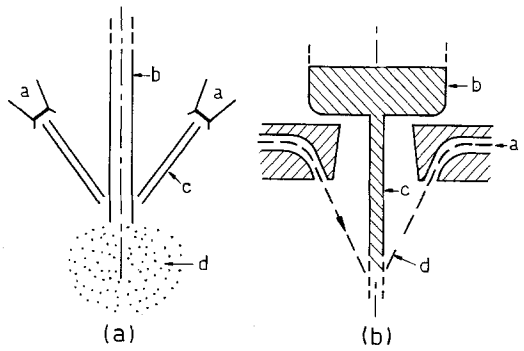

Figure 2 Representative gas-atomization configurations. (a) Two-jet configuration: a, jets; b, liquid-metal stream: c, gas stream; d, atomized powder. (b) Annular-ring configuration: a, ring orifice; b, liquid metal reservoir; c, liquid metal stream; d, gas stream [70–72].

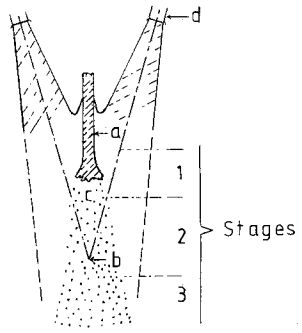

Figure 3 The three stages of liquid-metal stream disintegration in gas atomization. (a, liquid metal stream; b, focal point of gas streams; c, atomized powder; d, gas jets [75].

showing that the overall process consists of three stages (Fig. 3):

1. primary breakup of the liquid stream;
2. secondary disintegration of the molten droplets;
3. solidification of the particles.

In accordance with the model developed by Dombrowski and Johns [76], for the disintegration of a liquid sheet (Stage 1 in Fig. 3), See and Johnston [75] showed that the vacuum created around the metal stream, coupled with stream acceleration, leads to expansion of the metal stream into a diverging cone shape which is hollow. The hollow stream thins out and breaks into ligaments and sheets of thin liquid metal. The thin sheets and ligaments, of low surface tension, at high velocity, break into droplets of a wide range of powder sizes (Fig. 4).

It is important to note that actual atomization occurs above the point of focus of the gas stream (Fig. 3); this is because the vacuum created around the metal causes the liquid metal to expand into a hollow conical configuration of molten metal. Actual atomization then occurs at the circumferential periphery of the cone. The formation of a metal powder by gas atomization can then be described by the drawing shown as Fig. 5.

The following remarks may be made.

(a) As small, thin unstable sheets flying through space, they reform into round particles by folding, trapping the atomizing gas internally.

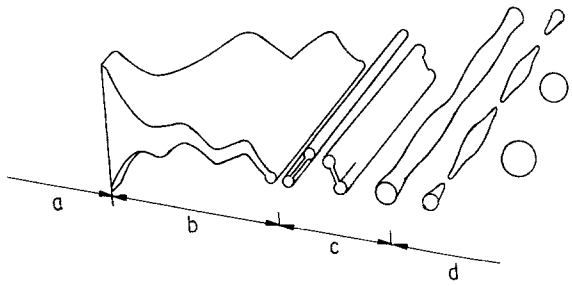

Figure 4 Model of the disintegration of a liquid sheet: a, stable sheet; b, growth of waves on sheet; c, fragmentation and formation of ligaments; d, breakdown of ligaments into drops. After Dombrowski and Johns [76].

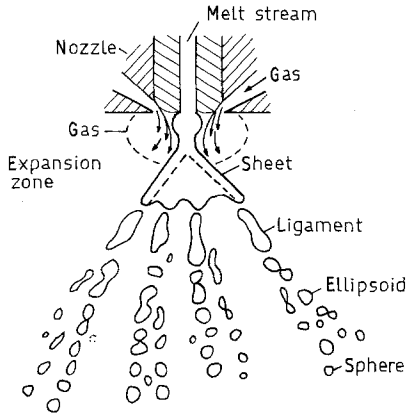

Figure 5 The formation of a metal by gas atomization [74].

(b) For alloys with alloying elements which readily oxidize to form refractory oxides, Al_2O_3 for example, the spheroidization into droplets is prevented or hindered and highly irregular powders and rough flakes form. Thus, the atmosphere in the atomizing chamber must be protective to minimize formation of thick refractory oxides.

2.1.2. Some defects in gas-atomized powders

The finer the powder the greater its reactivity with the various atmospheres it will encounter in subsequent processing to a fully dense structure. The purity and type of gas used for atomization or the working atmosphere are therefore very important. Clearly, inert gases should be preferred. The specific gas will also play a role in determining the solidification and cooling rate of the powder particles [68, 69].

Alloys based on or rich in elements which oxidize readily must be processed so as to limit contamination, which means minimizing surface area for a given powder lot size. In the case of aluminium alloys, there is danger of formation of hydrates on the surface. These hydrates, if formed, must be treated in the powder state at an appropriate temperature to decompose them. If the hydrate is incorporated into the hot-consolidated product, swelling will occur on subsequent solution heat treating or during high-temperature service. Oxide contents at levels of several tenths of a per cent (in aluminium) are not unknown for a significant number of powder-based alloys produced in air or in an oxidizing gas [68].

2.1.3. Gas porosity

Gas porosity (hollow powders) can be extremely detrimental to properties. All of the subsonic gas atomization processes tend to produce powder particles with entrapped gas; this is characteristic of the three-step atomization processes. In the as-hot extruded or as-HIPed (hot isostatically pressed) structures of gas containing particulates, one generally does not see the presence of trapped gases, but subsequent temperature exposure for solution heat treatment will cause swelling when the internal gas pressure exceeds the creep resistance of the alloy at the appropriate temperature [15, 77].

It can be concluded that the atomizing conditions for powders are the main reason for gas entrapment. However, one has to recognize that subsequent post-atomization handling and storage under a normal environment (in air) can also affect the surface conditions of the materials, mostly due to moisture effects.

2.1.4. Blistering

Surface blistering, illustrated in Fig. 6, is a form of damage to aluminium and aluminium alloy products, causing low and erratic yield. The basic cause is the inflation of internal defects by entrapped hydrogen when the overlying metal is soft during heat treatment. The effect is observed after final or intermediate annealing or after solution treatment preparatory to age hardening.

The solubility of hydrogen in solid aluminium at annealing or solution-treatment temperature is so low [78] that the residual dissolved hydrogen concentration in industrial products is always high enough to yield a disruptive pressure (Fig. 7). The incidence of blistering is therefore largely determined by the nature and distribution of internal defects.

2.2. Gases in metals

It is known that hydrogen and oxygen dissolve in atomic form in both liquid and solid metals. For the monoatomic noble gases (helium, neon, argon, etc.) one would expect a solubility proportional to the pressure. It turns out, however, that there is no metal in which they will dissolve to a measurable degree.

There are two main types of gases in liquid metals: (i) simple gases, i.e. the single gases like oxygen and hydrogen which dissolve in the liquid metal in their atomic form, O and H; (ii) complex gases, such as H_2O, which are formed by the reaction between elements present in the melt or moisture.

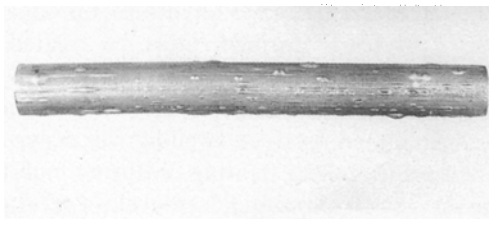

Figure 6 Extruded sample showing surface blistering after heat treatment.

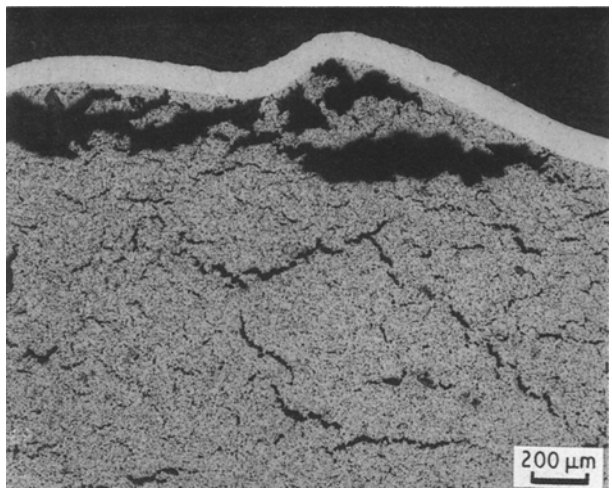

Figure 7 Effect of gas entrapment.

Complex gas formation often produces higher gas porosity levels than if the component gaseous elements were separately present in the melt. Reducing the level of oxygen in the liquid metal provides the best means of control of complex gas solution.

2.2.1. Hydrogen and oxygen in aluminium

2.2.1.1. Hydrogen. It is well known that hydrogen is the only gas with measurable solubility in aluminium [78–81]. Its solubility is small related to the solubility of hydrogen in many other metals. As is the case with gases in other metals, the problems encountered with gas in aluminium are due to the great difference in solubilities of hydrogen in liquid and solid metal at the freezing point. Values for the concentration in equilibrium with the gas at atmospheric pressure reported by different authors [78, 82–86] are given in Fig. 8.

The smoothed results yield for the liquid

$$\log S = -(2761/T) + 2.768 \quad (1)$$

and for the solid

$$\log S = -(2580/T) + 1.399 \quad (2)$$

where S is the solubility (cm^3) of hydrogen at standard conditions per 100 g metal. As shown in Fig. 8 [78, 82–86], aluminium in the liquid state can dissolve nearly 15 times as much hydrogen as in the solid state ($0.7\,cm^3/100\,g$ Al, compared with $0.04\,cm^3$, respectively).

The gas absorption and desorption reactions are frequently thermally activated processes and cannot proceed at high rates at lower temperatures, e.g. as a consequence of slow diffusion in the bulk.

Because during the solidification of the atomized powders the hydrogen (whether atomic or already recombined to molecular) will be at least partially trapped in the solidified particles, typically rounded hydrogen blowholes will form in the subsequently consolidated metallic powder (Fig. 9).

The presence of gas porosity in the powder is caused by the large change in gas solubility between the liquid and solid metal and the difficulty of removing this relatively large volume of gas at the solidification

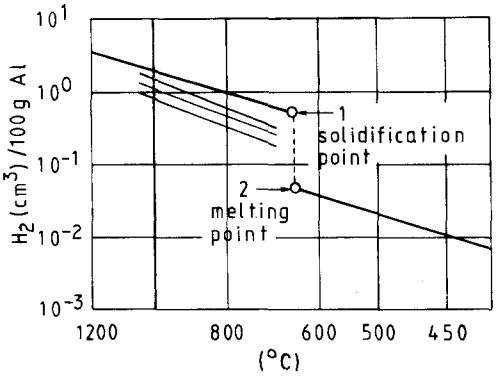

Figure 8 Solubility of hydrogen in aluminium and aluminium alloys as a function of temperature [78, 82–86].

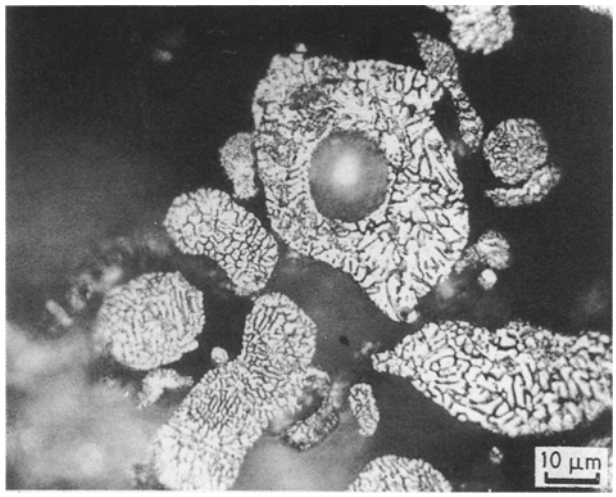

Figure 9 Metallic powder showing a rounded hydrogen blowhole.

front. A rapid rate of solidification increases the likelihood of gas entrapment during powder atomization. Simple gases dissolve in most metals by an endothermic reaction so that as the liquid-metal temperature increases, gas solubility increases. To minimize the problem, conditions tending to favour hydrogen pick-up must be avoided.

2.2.1.2. Oxygen. Aluminium reacts with oxygen either present in the protective atmosphere or formed by dissociation of water vapour to form Al_2O_3

$$\frac{4}{3}Al + O_2 \rightleftharpoons \frac{2}{3}Al_2O_3 \quad (3)$$

though more complex reactions are also possible, such as the formation of $AlO_x(OH)_{3-2x}$ (with $x = 0$ to 1.5).

The equilibrium constant, K_p, of Reaction 3

$$K_p = (p_{O_2})^{-1} = \exp(-\Delta G^\circ/RT) \quad (4)$$

represents the temperature dependence of the terminal solubility, where p_{O_2} is the partial pressure of oxygen, ΔG° is the standard Gibb's function and the other symbols have their usual meaning. In the aluminium–oxygen system the partial pressure of oxygen in equilibrium with Al_2O_3 is very small and far below the range attainable in vacuum systems. Under these conditions only oxidation can take place. Therefore, even at low residual oxygen pressures in ultra-high vacuum systems, the metal will be completely covered with an oxide layer.

2.3. Surface condition of powders after atomizing and keeping at room temperature

Aluminium alloy powder particles prepared by atomization contain a hydrated oxide layer with adsorbed water molecules formed during solidification and subsequent handling which according to the alloy composition has been described as an amorphous layer of Al_2O_3–$2Al(OH)_3$ and MgO–$Mg(OH)_2$ mixtures covered by a mixture of H_2O/O_2.

In Figs 10 and 11 an atomic concentration profile of the surface layer, as determined by Auger analysis, is given for the powders J1 (Al–20Si–3Cu–1Mg) and K1

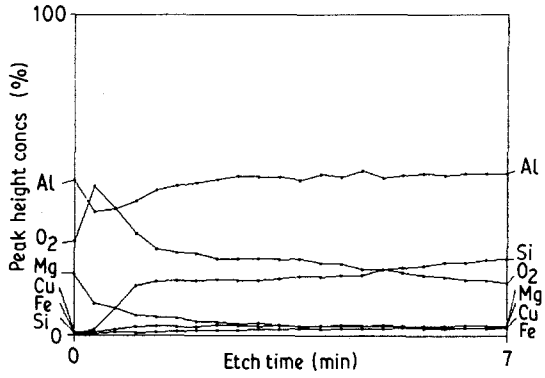

Figure 10 Atomic concentration depth profile for the air atomized Al–20Si–3Cu–1Mg powder J1 [68].

(Al–20Si–5Fe–2Ni) [68]. In powder K1, which contains no magnesium, the oxide surface layer consists of aluminium (hydro)oxides. A hydrogen profile cannot be determined by Auger measurements. Powder J1, which contains 1% magnesium, has a surface layer of mixed aluminium and magnesium (hydro)oxides. Because of the large affinity of magnesium to oxygen the surface layer is highly enriched in magnesium, as can be seen in Fig. 10.

2.4. Theory of degassing of aluminium alloy powders

If hydrogen and water vapour have to be removed at a noticeable rate from solid powders, by vacuum heat treatments, the corresponding pressures of the gas species formed at the degassing temperature must be relatively high. Pressure data of hydrogen and H_2O (and oxygen) are obtained from the degassing experiments. In the absence of reliable data they can be estimated from the standard Gibbs function, ΔG°, of the formation of metal–nonmetal compounds being in equilibrium with the solid metallic solution. In degassing reactions molecular oxygen is released only from some noble metals [87]. However, in many cases the pressure of volatile oxides is several orders of magnitude higher than the oxygen pressure. Whether the optimum degassing temperature should be chosen

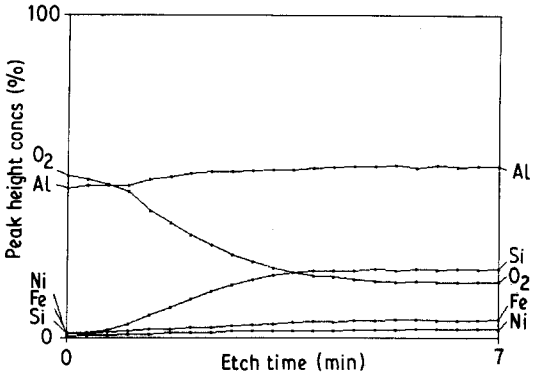

Figure 11 Atomic concentration depth profile for the air atomized Al–20Si–5Fe–2Ni powder K1 [68].

high or low, depends on the heat of solution, $\Delta H°$, of the corresponding gaseous species. If it is negative, i.e. for exothermic reactions, the gas pressure at constant concentrations rises with rising temperature, and annealing treatments at higher temperatures become more effective.

The conditions for optimization of degassing treatments are not described completely by equilibrium data because they can determine only the direction of the reaction under the conditions chosen and the final gas content attainable after sufficiently long degassing times. The kinetics of the processes are also of high importance. An absolute rate-limiting factor in vacuum metallurgical degassing processes is the amount of gas that can be released from the powder surface due to the equilibrium pressures of volatile components. The maximum concentration decrease of a piece of material attainable in a degassing treatment is given approximately by the relation [88].

$$\Delta c \approx \frac{1}{2}\frac{pt}{d} \tag{5}$$

where Δc is the change in concentration of dissolved species (in at %), p is the gas equilibrium pressure (mbar), t is the degassing time (sec) and d is the thickness of the material (cm).

Another rate-limiting factor for the degassing of metals in the solid state is the diffusion of dissolved gas atoms to the surface [89]. Other effects that can decrease the degassing rate drastically are thermally activated processes on the surface, such as formation and evaporation of gas molecules.

According to the theoretical treatment of Litvintsev and Arbuzova [17], during the degassing of powders of pure aluminium or magnesium-free aluminium alloys on heating from room temperature to 550 °C, the following reactions take place:

(i) removal of absorbed water vapour

$$Al_2O_3{\cdot}3H_2O + H_2O_{ads} \rightarrow Al_2O_3{\cdot}3H_2O + H_2O \tag{6}$$

(ii) during heating in vacuum the hydroxides of the surface oxide layer react to form several modifications of aluminium trihydroxide ($Al_2O_3{\cdot}3H_2O$) whose decomposition (dehydration) stages can be represented by

$$Al_2O_3{\cdot}3H_2O \xrightarrow[150 \text{ to } 175\,°C]{} Al_2O_3{\cdot}2.5H_2O \tag{7}$$

$$Al_2O_3{\cdot}2.5H_2O \xrightarrow[310 \text{ to } 500\,°C]{} Al_2O_3{\cdot}H_2O \tag{8}$$

$$Al_2O_3{\cdot}H_2O \xrightarrow[> 500\,°C]{} \gamma\text{-}Al_2O_3 \tag{9}$$

These transformations take place gradually over ranges of increasing temperatures as confirmed by the representations of phase relations in the $Al_2O_3{\cdot}H_2O$ system (Fig. 12) and the transformation sequence $Al(OH)_3 \rightarrow Al_2O_3$ (Fig. 13) [90]. There are two routes the decomposition of $Al(OH)_3$ can take (Fig. 14) [91]. Our experimental conditions of degassing favour path a in Fig. 14. These conditions tend to keep water vapour within the crystal long enough for AlOOH (boehmite) formation.

When water vapour comes into contact with an oxide-free aluminium surface, the reaction

$$2Al + 3H_2O \rightarrow Al_2O_3 + 3H_2 \tag{10}$$

takes place, which is the principle source of hydrogen evolution. Small amounts of hydrogen may be freed by desorption from the surface of the powder of absorbed or solved hydrogen, which occurs at the lower temperatures.

The situation is complicated, in the case of the alloy J1, by the presence of highly mobile and reactive magnesium in the form of $Mg(OH)_2$ or $MgAl_2O_4$ (crystalline) which are more stable than the aluminium (hydro)oxides.

$$Mg + H_2O \rightarrow MgO + H_2 \tag{11}$$

$$Al_2O_3 + MgO \rightarrow MgAl_2O_4 \tag{12}$$

Dehydration of aluminium is a non-reversible process but at the same time, we have desorption of water from the surface (reversible process) and when the temperature is high enough (over 400 °C), a stronger interaction must take place between water and the alloy probably due to oxide break up releasing hydrogen (Equations 10 and 11). In addition to hydroxides, $Al(OH)_3$ and $Mg(OH)_2$, physically adsorbed gases (H_2O and oxygen) constitute the powder surface oxide layer. Considering that a part of the oxygen in aluminium hydroxides is used to form Al_2O_3, the main source of the reduced oxygen level may be the physically adsorbed gases. A part of the physically adsor-

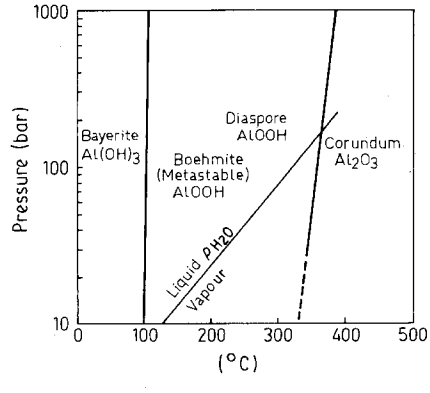

Figure 12 Phase diagram Al_2O_3–H_2O.

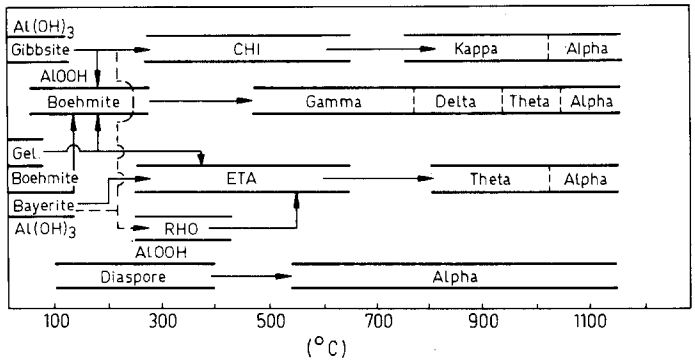

Figure 13 Transformation sequence $Al(OH)_3 \rightarrow Al_2O_3$.

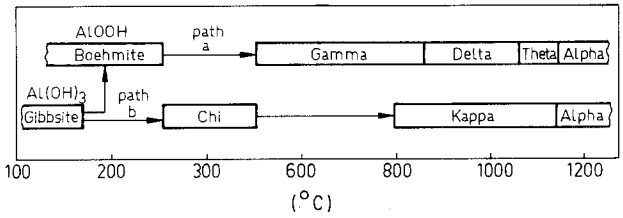

Figure 14 Routes for decomposition of $Al(OH)_3$.

bed water will also participate to form additional oxides.

After some thermodynamical consideration, it is apparent that the principal chemical reactions governing the degassing process are

$$\frac{1}{3}Al_2O_3 \cdot 3H_2O \rightarrow \frac{1}{3}Al_2O_3 + H_2O \quad (13)$$

$$\frac{4}{3}Al + O_2 \rightarrow \frac{2}{3}Al_2O_3 \quad (14)$$

$$\frac{2}{3}Al + H_2O \rightarrow \frac{1}{3}Al_2O_3 + H_2 \quad (15)$$

$$2Mg + O_2 \rightarrow 2MgO \quad (16)$$

$$Mg + H_2O \rightarrow MgO + H_2 \quad (17)$$

3. Experimental procedure

The powders chosen for investigation consisted of two lots of rapidly solidified P/M aluminium alloys, atomized in air, based on the hypereutectic Al–Si–X system containing 20 wt % Si: powder J1 produced by the Japanese firm Showa Denko K.K., with an average particle size of 16 to 24 μm [68], and powder K1 produced by the West German firm Eckart-Werke, with an average particle size of 8 to 16 μm [68]. The powder J1 belongs to a heat-treatable group while the powder K1 belongs to a non-heat-treatable group. Experiments were aimed at recording mainly moisture and hydrogen desorption as a function of temperature. The chemical compositions of these P/M alloys, as obtained by atomic absorption spectrophotometry, are shown in Table I [68].

The oxygen content of the powders was measured using a Strohlein OSA-MAT analyser by reducing the oxides on heating them in the presence of carbon [68].

The hydrogen content was measured at 550 °C, by an H-mat 251 Strohlein analyser using a standard

TABLE I Chemical composition (wt %) of rapidly solidified powders [68]

Powder	Si	Cu	Mg	Fe	Ni	O_2	Al
J1	18.8	3.22	1.18	0.25	–	0.20	bal.
K1	19.3	–	–	4.82	2.06	0.21	bal.

procedure [92] providing the following results:

	H	H_2
Powder J1	24.58 p.p.m.	27.53 $cm^3/100\,g$
Powder K1	13.09 p.p.m.	14.66 $cm^3/100\,g$

The hydrogen content for the air-atomized aluminium powders is 50 to 100 times higher than that for degassed cast alloys. The threshold value of hydrogen content for degassed cast aluminium alloys, for general applications, is reported to be 0.30 $cm^3/100\,g$ [92] while degassed ingots of the highest quality are characterized by even lower hydrogen content, 0.05 to 0.10 $cm^3/100\,g$ [83]. From these data the conclusion must be drawn that practically all hydrogen is contained by the oxide layer in the form of chemically or physically bound H_2O, which is reduced, in the gas analyser, to molecular hydrogen by Reaction 10.

The first processing step applied in this work, for degassing measurements, concerned cold precompaction of the loose powdered aluminium alloys into cans. The precompaction was carried out on a uniaxial hydraulic press with a rigid die. The compaction pressure of 160 MPa was used in order to provide a material of about 65% theoretical density, leaving a proper level of interconnected porosity to allow subsequent degassing to occur efficiently. Each can contained ~ 300 g aluminium powder after compaction. A cover plate with an evacuation tube was welded to the end of the can and the evacuation tube was connected to a vacuum source (turbomolecular pump connected to a quadrupole mass spectrometer). The cans and evacuation tubes were made of 6063 (Al–0.4Si–0.7Mg) aluminium alloy. For canned powders, extensive work was succesfully undertaken to ensure that the vacuum was maintained after the can had been sealed [93].

The vacuum degassing experiments were carried out, in the temperature range 20 to 550 °C, in a horizontal furnace heated at ~ 2.5 °C min^{-1}. For simplicity, a complete degassing analysis of only one of the powders is presented, namely the air-atomized

Al–20Si–3Cu–1Mg powder J1, although some important results of the powder K1 are also included for comparison. The partial pressures of the released gases were monitored and analysed during the heating phase by a computerized Edwards EQ80F residual gas analyser (RGA). Temperatures in different locations of the can were simultaneously recorded. The unit measures total vacuum pressure and analyses the partial pressures over the mass range 1 to 80 a.m.u. (atomic mass units); the sensor being a quadrupole mass spectrometer.

It is important to point out the concept of partial pressure used in this work. Partial pressure is the pressure arising from a single ion mass value or from a given gas molecule type. The partial pressure readings shown are the values corresponding to ion mass values representative of given molecules. For example, $M = 18$ a.m.u. peaks are often displayed as arising from H_2O and vice versa, although the fingerprint for water contains other peaks at 17, 16 and 2 a.m.u. The analyser itself is equipped with twin filaments and is an improved version of the proven Anavac.

4. Results and discussion

4.1. Continuous degassing

Two samples of different composition Al–20Si–3Cu–1Mg (powder J1) and Al–20Si–5Fe–2Ni (powder K1) were heated independently up to 550 °C at a rate of $\sim 2.5\,°C\,min^{-1}$, under high vacuum. The partial pressures of moisture (H_2O) and hydrogen as a function of temperature were recorded. These degassing products are evaporated from physisorbed water and decomposed hydroxides from the surface layer.

Figs 15 and 16 show the respective mass spectrums generated by the residual gas analyser. These spectrums show the relative amounts of H_2O and hydrogen evolved and the temperature ranges over which each is given off. Both P/M aluminium alloys show similar degassing curves in that a large water and hydrogen desorption can be noticed with peaks at different temperatures. As expected, emission of H_2O was dominant at lower temperatures.

From those results it can be seen that particularly vigorous H_2O desorption occurs in the temperature ranges 50 to 370 and 50 to 300 °C for the powders J1 and K1, respectively. We can say that at those final temperatures equilibrium is established between the

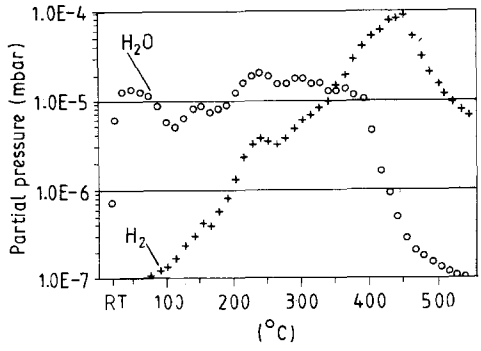

Figure 15 Powder J1 (Al–20Si–3Cu–1Mg) degassed continuously up to 550 °C.

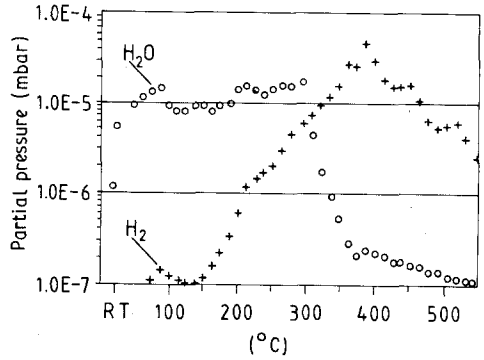

Figure 16 Powder K1 (Al–20Si–5Fe–2Ni) degassed continuously up to 550 °C.

rate of moisture liberation and the rate of evacuation. Thus, 370 and 300 °C represent the temperature threshold of active moisture liberation from the powders J1 and K1, respectively. Above those values the descending portions of the moisture evolution curves indicate that most of the water vapour, which is released above these temperatures, is converted into hydrogen by Reaction 10.

The release of hydrogen from the powder shows a quite different pattern as a function of temperature. Hydrogen production starts at about 70 °C and gradually increases to a maximum at about 450 °C for powder J1 and 380 °C for powder K1. These maxima coincide with the strong decreases in H_2O partial pressure. A secondary local maximum in the hydrogen partial pressure is found at ~ 240 °C in J1 and at ~ 220 °C in K1. These local maxima correspond to local maxima in the H_2O partial pressure curves. It is evident from Figs 15 and 16 that the H_2O evolution starts at room temperature before hydrogen release takes place.

Whereas the process of moisture liberation during the heating of the powders J1 and K1, under high vacuum, is associated with the phenomenon of desorption and decomposition of aluminium hydroxide modifications, the evolution of hydrogen over the relatively wide ranges of temperatures where it was observed to occur, can only be attributed to the reaction between moisture and aluminium [17] or magnesium [94] according to Reactions 10 and 11. As can be deduced from Fig. 15, the evolution of hydrogen is particularly dangerous for heat-treatable P/M aluminium alloys (solution heat-treatment temperature 470 °C over 1.5 h) and P/M materials which serve at elevated temperature (~ 200 to 400 °C), therefore those P/M materials must be degassed to remove moisture and hydrogen prior to consolidation and heat treatment, providing in such a way a non-porous product without blistering.

The maxima of hydrogen evolution at 450 °C (powder J1) and 380 °C (powder K1) correspond to the transformation of aluminium monohydroxide into aluminium oxide. The small maxima at the lower temperatures 240 °C (powder J1) and 220 °C (powder K1) correspond to the transformation of $Al(OH)_3$ into AlOOH (Fig. 14). The end products of the degassing process are amorphous Al_2O_3 and crystalline MgO particles formed according to the reactions described

above. Because hydroxides are eliminated, degassing increases the volume ratio between crystallites and amorphous constituents in the film.

Comparing powder J1 and powder K1 during degassing (Figs 15 and 16), a difference of about 70 °C between maximum temperatures for both the release of water (370 °C for J1 and 300 °C for K1) and for the release of hydrogen (450 °C for J1 and 380 °C for K1) is found. The relatively higher amounts of water and of hydrogen shown by the powder J1 are attributed, on the one hand, to its higher surface oxide thickness (44 nm on average) in comparison with 34 nm on average for the powder K1 [68]; on the other, as reported by Estrada and Duszczyk [68], a comparison of the chemical composition of the surface oxide films indicated that the surface layer of the powder J1 was rich in the more stable magnesium (hydro)-oxide, $(Mg(OH)_2)MgO$, while that of the powder K1 was nearly pure in aluminium (hydro)oxide, $(Al(OH)_3)Al_2O_3$, as shown by their atomic concentration depth profiles, illustrated in Figs 10 and 11, respectively.

Solid state degassing depends on (a) a pressure lower than the equilibrium pressure to enable the surface reactions to occur, and (b) a temperature high enough to enable the gas to diffuse to the free surface of the oxide layers. However, the thermodynamics and kinetics of the breakdown which are needed in order to determine a suitable combination of pressure and temperature, are not known so far.

Because a main objective of our research concerns the understanding of hydrogen evolution, during degassing of Al–20Si–X P/M alloys, attributed to the reaction between moisture and aluminium [17] or magnesium [94], let us consider the fundamental aspects (a and b) mentioned above.

(a) Surface reactions. A thermodynamical approach in terms of the free energy change, ΔG, applied to some of the principal chemical reactions (Section 2.4) is described below.

Under normal conditions water release takes place according to the reactions

$$\frac{2}{3}Al(OH)_3 \rightarrow \frac{1}{3}Al_2O_3 + H_2O \qquad (18)$$

where $p_{H_2O} = 1$ atm at a temperature of ~ 81 °C (354 K), and

$$Mg(OH)_2 \rightarrow MgO + H_2O \qquad (19)$$

where $p_{H_2O} = 1$ atm at a temperature of ~ 258 °C (531 K).

These results show that $Mg(OH)_2$ is much more stable than $Al(OH)_3$ which explains the higher temperatures for the release of water and formation of hydrogen in the magnesium-containing hydroxide layers of powder J1 in contrast with the magnesium-free hydroxide layer of powder K1.

The combination of water vapour with aluminium proceeds according to the Reaction 15 whose free energy is [95] $\Delta G = -75\,380 + 14.34\,T$ cal mol^{-1}.

According to the laws of thermodynamic equilibrium [96, 97]

$$\ln K = -(\Delta G/RT) \qquad (20)$$

and

$$K = [p_{H_2}(a_{Al_2O_3})^{1/3}]/[p_{H_2O}(a_{Al})^{2/3}] \qquad (21)$$

where K is the equilibrium constant of the reaction, R the universal gas constant, T the absolute temperature, and a the activity.

After standard calculations [95], the following relations are obtained

$$K = 1.09 \times 10^{41} \quad (\text{for } T = 100\,°C) \qquad (22)$$

$$K = 1.52 \times 10^{18} \quad (\text{for } T = 500\,°C) \qquad (23)$$

When these results are compared with the experimental data shown in Figs 15 and 16 it must be concluded that the activity of the aluminium atoms is very low at the hydroxide surface layer. Then, if it is assumed that $Al_2O_3 \approx 1$, the activity of aluminium, a_{Al}, must be of the order of 10^{-64} to 10^{-24}.

The reaction for the conversion of H_2O by aluminium described above competes with Reaction 14 for the binding of free aluminium at the powder surface. The free energy of this reaction is [95] $\Delta G = -266\,000 + 49.9\,T$ cal mol^{-1} and

$$K = [(a_{Al_2O_3})^{2/3}]/[p_{O_2}(a_{Al})^{4/3}] \qquad (24)$$

from which

$$K \approx 10^{145} \quad (\text{for } T = 100\,°C) \qquad (25)$$

$$K \approx 10^{64} \quad (\text{for } T = 500\,°C) \qquad (26)$$

From this result, it can be concluded that:

1. as long as sufficient free oxygen is present in the system, Reaction 15 for the conversion of H_2O will not take place; and

2. the activity of aluminium, a_{Al}, in the powder surface must be extremely low. Thermodynamical data were taken from the work of Barin and Knacke [95].

(b) Diffusion. Let us consider the diffusion of aluminium through an Al_2O_3 layer, ~ 40 nm thick [68]. The presence of this oxide layer (barrier) between the parts participating in the diffusion should affect the diffusion coefficient. However, as shown by Lundy and Murdock [98], for tracer ^{26}Al diffusion the barrier effects at temperatures above 600 °C were not present. At lower temperatures the effects were small and are not believed to affect significantly the results. Then, it is possible to use the self-diffusion coefficient of aluminium also for the diffusion of aluminium through the oxide layer.

The equation describing the diffusion coefficient of ^{26}Al in aluminium as function of temperature is

$$D_{^{26}Al} = 171 \exp(-34\,000/RT) \qquad (27)$$

the constants $D_0 = 171$ mm^2 sec^{-1} and $Q = 34$ kcal mol^{-1} are taken from the work of Lundy and Murdock [98]. The temperature-diffusion data are summarized in Table II. With these values it is possible to estimate the flux of aluminium through the oxide layer by means of Fick's first law

$$J = -D\frac{dc}{dx} \qquad (28)$$

TABLE II Diffusion coefficients of ^{26}Al in aluminium

Temperature (°C)	D_{Al} ($mm^2\,sec^{-1}$)
RT	1.97×10^{-23}
100	2.04×10^{-18}
200	3.32×10^{-14}
300	1.83×10^{-11}
400	1.55×10^{-9}
500	4.16×10^{-8}

where D is the diffusion coefficient ($mm^2\,sec^{-1}$), and dc/dx the concentration gradient of aluminium through the oxide layer ($mol\,mm^{-2}\,mm^{-1}$).

Table III gives the number of atoms of aluminium diffusing through an oxide layer, 40 nm thick, at different temperatures. If the mean particle size of the powder J1 is taken as 24 μm [68], the volume per particle is 7.24×10^3 μm^3 which gives 15.8×10^9 particles in the can (~ 300 g powder at ~ 65% theoretical density) with a total surface of 28.6×10^6 mm^2. Table IV gives the number of aluminium atoms coming to the surface, per second, at different temperatures.

By means of the generalized gas law ($PV = nRT$) it is possible to estimate the amount of molecules of H_2O and oxygen contained in a gas system volume of ~ 1 litre, (a) at room temperature and (b) 500 °C.

(a) Room temperature. With p_{H_2O} (298) = 10^{-9} atm and $p_{O_2}(298) = 10^{-12}$ atm, which are taken from the degassing experiments, we get $n_{H_2O} = 2.5 \times 10^{13}$ mol H_2O and $n_{O_2} = 2.5 \times 10^{10}$ mol O_2, while 5×10^5 atoms of aluminium are coming to the powder surface in 1 h.

From these results it is apparent that the affinity of oxygen for aluminium is greater than the affinity of H_2O for aluminium, which is in agreement with the thermodynamic data given before. We can also conclude that at room temperature no new hydrogen is formed, and that the hydrogen which appeared must have been solved or absorbed in the powder.

(b) Elevated temperature (500 °C). The number of atoms (10^{21}) of aluminium coming to the powder surface at 500 °C in 1 h is more than enough to tie up 2.5×10^{10} molecules of oxygen. Bearing in mind that only 4×10^{10} aluminium atoms are necessary to tie up this number of oxygen molecules the rest can be used for the reaction with H_2O.

The total number of H_2O molecules present originally in the system was 3.6×10^{22} which means that Reaction 10 can go to completion at 500 °C in a couple of hours. Between 150 and 300 °C the number of aluminium atoms arriving at the surface becomes sufficiently large to bind the oxygen atoms and the formation of hydrogen can start (Fig. 16), whilst at about 400 °C all H_2O is transformed to hydrogen.

Thus, it is apparent that the temperature is the principal parameter which influences the degassing behaviour. It appears, from this semi-quantitative approach, that the diffusion of aluminium through the oxide layer can explain, to a large extent, the kinetics of the degassing of aluminium powders.

It appears, from the thermodynamical data, that $MgAl_2O_4$ and MgO are more stable than Al_2O_3.

TABLE III Flux of aluminium atoms through an oxide layer of 40 nm

Temperature (°C)	J_{Al} (at. $mm^{-2}\,sec^{-1}$)
RT	4.92×10^{-6}
100	5.10×10^{-1}
200	8.30×10^{3}
300	4.57×10^{6}
400	3.87×10^{8}
500	1.04×10^{10}

TABLE IV Number of aluminium atoms coming to the surface

Temperature (°C)	(at. sec^{-1})
RT	141×10^{0}
100	146×10^{5}
200	237×10^{9}
300	131×10^{12}
400	111×10^{14}
500	30×10^{16}

Thus magnesium can reduce Al_2O_3 to form $MgAl_2O_4$ or MgO depending on the relative abundance of the elements. It can be said that after the initial formation of a thin layer of amorphous Al_2O_3, magnesium diffuses through that layer until the surface is completely covered by crystalline MgO. Because the alloy K1 does not contain any magnesium, its surface oxide film is predominantly rich in Al_2O_3. This indicates that, according to thermodynamics, the strong effect of magnesium as an alloying element is the main reason for the shifting of both the release of moisture and the release of hydrogen toward higher temperatures.

5. Conclusions

1. The fundamental aspects of moisture and gas evolution during degassing of a porous billet can be described in a semi-quantitative manner using a thermodynamical approach.

2. During degassing of Al–20Si–X P/M alloys, at temperatures up to 550 °C, the partial pressures of moisture and hydrogen were within the range 10^{-4} to 10^{-7} mbar (1 bar = 10^5 Pa).

3. The thermodynamics of gas desorption is mainly influenced by temperature which is the critical degassing parameter.

4. It appears, from the semi-quantitative approach, that the diffusion of aluminium through the oxide layer can explain, to a large extent, the kinetics of degassing of aluminium powders.

5. A shift of the release of moisture and hydrogen towards higher temperatures is due to the presence of MgO in the surface layer compared to those when only Al_2O_3 builds the oxide film. It has been proved, by a thermodynamical approach, that the reaction of magnesium with water vapour proceeds more intensely than that between aluminium and water vapour.

Acknowledgements

The authors thank T. L. J. de Haan and W. Weerheijm for skilful assistance with the experiments, Mr G. van Slingerland for making the drawings, Mr A. M. J. W. Bakker for providing the micrographs, Mr W. A. J. Brabander for welding the cans, and Drs J. Bruining, Th. W. de Loos and L. Kowalski for helpful discussions. The financial support of the National Polytechnic Institute in Mexico (IPN), and the Royal Academy of Science in the Netherlands (KNAW), the Foundation for Technological Research (STW) and the Foundation for Fundamental Research of Matter (FOM) is gratefully acknowledged.

References

1. N. KUROISHI, Y. ODANI and Y. TAKEDA, *Metal Powder Report* **40** (1985) 642.
2. T. HIRANO, F. OHMI, S. HORIE, F. KIYOTO and T. FUJITA, in "Proceedings on Rapidly Solidified Materials", San Diego, February 1986, edited by P. W. Lee and R. S. Carbonara (American Society for Metals, Metals Park, Ohio, 1986) p. 327.
3. T. HIRANO, T. UI and F. OHMI, in "Proceedings of the 31st International SAMPE Symposium, Los Angeles, California, 1986, edited by J. L. Bauer and R. Dunaetz (SAMPE, California, 1986) p. 1655.
4. K. AKECHI, Y. ODANI and N. KUROISHI, *Sumitomo Electric Tech. Rev.* 24 (January 1985) 191.
5. S. K. DAS, *Int. J. Powder Metall.* **24** (1988) 175
6. T. G. NIEH, R. A. RAINEN and D. J. CHELLMAN, in "Proceedings of the Fifth International Conference on Composite Materials, San Diego, August 1985, edited by W. C. Harrigan Jr, J. Strife and A. K. Dhingra (The Metallurgical Society of AIME, Warrendale, Pennsylvania, 1985) p. 825.
7. V. ARNHOLD and K. HUMMERT, in "Proceedings on Dispersion Strengthened Aluminium Alloys", Phoenix, January 1988, edited by Y-W. Kim and W. M. Griffith (TMS, Warrendale, Pennsylvania, 1988) p. 483.
8. J. F. FAURE and L. ACKERMANN, *ibid.* p 501.
9. J. A. HAWK, P. K. MIRCHANDANI, R. C. BENN and H. G. F. WILSDORF, *ibid.* p. 517.
10. J. J. LEWANDOWSKI, C. LIU and W. H. HUNT Jr, in 'Proceedings on Processing and Properties for Powder Metallurgy Composites", Denver, February 1987, edited by P. Kumar, K. Vedula and A. Ritter (The Metallurgical Society of AIME, Warrendale, Pennsylvania, 1988) p. 117.
11. H. J. RACK, *ibid.* p. 155.
12. M. W. MAHONEY, M. KENDING, A. R. MURPHY, M. R. MITCHELL and A. K. GHOSH, in "Proceedings of International Conference on PM Aerospace Materials, Luzern, November 1987 (Metal Powder Report, Shrewsbury, 1988) Paper no. 33.
13. I. YAMAUCHI, I. OHNAKA, S. KAWAMOTO and T. FUKUSAKO, *Trans. Jpn Inst. Metals* **27** (1986) 195.
14. J. L. ESTRADA, J. DUSZCZYK and R. YOSHIMURA, in "Proceedings of the 7th International Conference on Metrology, Automatization, Fine Mechanics, New Materials-Mikronika '87", Warsaw, November 1987, edited by L. Kudla and J. Lemanowicz (SIMP, Warsaw, 1987) p. 206.
15. J. L. ESTRADA, J. DUSZCZYK, B. M. KOREVAAR and R. YOSHIMURA, in "Proceedings of the 4th International Symposium on Science and Technology of Sintering", Tokyo, November 1987, edited by S. Sōmiya, M. Shimida, M. Yoshimura and R. Watanabe (Elsevier Applied Science, London, 1988) p. 581.
16. J. DUSZCZYK and J. L. ESTRADA, in "Proceedings of the Australian Bicentennial International Congress in Mechanical Engineering – New Materials and Processes for Mechanical Design", Brisbane, May 1988 (Institution of Engineers, Australia, 1988) Publication no. 88/4, p. 96.
17. A. I. LITVINTSEV and L. A. ARBUZOVA, *Sov. P/M Met. Cer.* **1** (1967) 1.
18. F. J. GURNEY, D. J. ABSON and V. Dé PIERRE, *Powder Metall.* **17** (33) (1974) 46.
19. J. P. LYLE and W. S CEBULAK, *Met. Trans.* **6A** (1975) 685.
20. J. P. H. A. DURAND, R. M. PELLOUX and N. J. GRANT, *Mater. Sci. Engng.* **23** (1976) 247.
21. W. S. CEBULAK, in "Proceedings of the International Conference on Rapid Solidification Processing", Reston, November 1977, edited by R. Mehrabian, B. H. Kear and M. Cohen (Claitor's, Baton Rouge, Louisiana, 1978) p. 324.
22. J. R. PICKENS, *J. Mater. Sci.* **16** (1981) 1437.
23. O. HUNDERI and T. SAVE, *Scand. J. Metall.* **10** (1981) 231.
24. J. T. MORGAN, H. L. GEGEL, S. M. DORAIVELU, L. E. MATSON, I. A. MARTORELL and J. F. THOMAS Jr, in "Proceedings on High Strength Powder Metallurgy Aluminium Alloys", Dallas, February 1982, edited by M. J. Koczak and G. J. Hildeman (The Metallurgical Society of AIME, Warrendale, Pennsylvania, 1982) p. 193.
25. V. A. PHILLIPS, *ibid.* p. 391.
26. R. YEARIM and D. SHECHTMAN, *Met. Trans.* **13A** (1982) 1891.
27. F. H. FROES and J. R. PICKENS, *J. Metals* **36** (January 1984) 14.
28. P. D. LIDDIARD, *Powder Metall.* **27** (1984) 193.
29. D. J. SKINNER and K. OKAZAKI, *Scripta Metall.* **18** (1984) 905.
30. Y-W. KIM, W. M. GRIFFITH and F. H. FROES, ASM Metals/Materials Technology Series, No. 8305-48 (American Society for Metals, Metals Park, Ohio, 1984) p. 1.
31. G. STANIEK, *Aluminium*, **60** (12) (1984) 3.
32. L. ACKERMANN, I. GUILLEMIN, R. LALAUZE and C. PIJOLAT, in "High strength powder metallurgy aluminium alloys", AIME Conference, Toronto, October 1985 (The Metallurgical Society of AIME, Warrendale, Pennsylvania, 1986) p. 175.
33. S. D. KIRCHOFF, J. Y. ADKINS, W. M. GRIFFITH and I. A. MARTORELL, in "Proceedings on Rapidly Solidified Powder Aluminium Alloys", Philadelphia, April 1984, edited by M. E. Fine and E. A. Starke Jr (ASTM, Philadelphia, Pennsylvania, 1986) p. 354.
34. J. MEUNIER, *ibid.* p. 260.
35. W. M. GRIFFITH, Y-W. KIM and F. H. FROES, *ibid.* p. 283.
36. Y-W. KIM and W. M. GRIFFITH, *ibid.* p. 485.
37. D. RAYBOULD and C. F CLINE, in "Proceedings on Rapidly Solidified Crystalline Alloys", Morristown, May 1985, edited by S. K. Das, B. H. Kear and C. M. Adam (The Metallurgical Society of AIME, Warrendale, Pennsylvania, 1985) p. 111.
38. O. BOTSTEIN, E. Y. GUTMANAS and A. LAWLEY, *Prog. Powder Metall.* **41** (1985) 123.
39. P. R. BRIDENBAUGH, W. S. CEBULAK, F. R. BILLMAN and G. H. HILDEMAN, *Light Metal Age* (October 1985) 18.
40. Y-W. KIM, W. M. GRIFFITH and F. H. FROES, *J. Metals* **37** (1985) 27.
41. V. A. PHILLIPS, *Metallogr.* **19** (1986) 265.
42. J. C. Le FLOUR, E. ANDRIEU and Y. BIENVENU, in "Proceedings of the International Powder Metallurgy Conference The Future of Powder Metallurgy P/M 86", Düsseldorf, July 1986, edited by W. A. Kayser and W. J. Hupmann (Verlag Schmid, Freiburg, 1986) p. 759.
43. M. J. COUPER and R. F. SINGER, in "Proceedings on Processing of Structural Metals by Rapid Solidification", Orlando, October 1986, edited by F. H. Froes and S. J. Savage (ASM International, Metals Park, Ohio, 1986) p. 273.
44. R. L. BYE, N. J. KIM, D. J. SKINNER, D. RAYBOULD and A. M. BROWN, *ibid.* p. 283.
45. S. D. KIRCHOFF and Y-W. KIM, *ibid.* p. 297.
46. Y-W. KIM and F. H. FROES, *ibid.* p. 309.
47. G. H. NARAYANAN, W. H. GRAHAM, W. E. QUIST, A. L. WINGERT and T. M. RONALD, *ibid.* p. 321.
48. M. P. THOMAS, I. G. PALMER and C. BAKER, *ibid.* p. 337.
49. O. BOTSTEIN, E. Y. GUTMANAS and D. ZAK, *ibid.* p. 961.
50. Y-W. KIM, in "Progress in Powder Metallurgy", Vol. 43 (MPIF, Princeton, NJ, 1987) p. 13.

51. R. D. SCHELLENG, in "Proceedings of International Conference on PM Aerospace Materials", Luzern, November 1987 (Metal Powder Report, Shrewsbury, 1988) Paper 23.
52. H C. ANGUS and G. R. D. SHRIMPTON, *ibid.* Paper 24.
53. J. BECKER, G. FISCHER, R. FURLAN and W. KEINATH, *ibid.* Paper 25.
54. M. J. COUPER, M. NAUER, R. BAUMANN and R. F. SINGER, *ibid.* Paper 28.
55. M. W. KEARNS, B. W. H. LOWE, C. B. BALIGA, P. TSAKIROPOULOS and R. W. GARDINER, *ibid.* Paper 30.
56. H. SCHLICH, M. THUMANN and G. WIRTH, *ibid.* Paper 31.
57. P. JOLY, P. LASNE, C. LEVAILLANT and P. BAUDUIN, *ibid.* Paper 32.
58. K. WEFERS and F. A. MOZELEWSKI, *Aluminium* **64** (3) (1988) 295.
59.. Y-W. KIM, in "Proceedings of the six-session on Dispersion Strengthened Aluminium Alloys", Phoenix, January 1988, edited by Y-W. Kim and W. M. Griffith (TMS, Warrendale, Pennsylvania, 1988) p. 157.
60. D. RAYBOULD, *ibid.* p. 199.
61. I. G. PALMER, M. P. THOMAS and G. J. MARSHALL, *ibid.* p. 217.
62. G. M. PHARR, M. S. ZEDALIS, D. J. SKINNER and P. S. GILMAN, *ibid.* p. 309.
63. S. F. CLAEYS, J. W. JONES and J. E. ALLISON, *ibid.* p. 323.
64. Y-W. KIM and F. H. FROES, *Aluminium* **64** (10) (1988) 1035.
65. V. CHIAVAZZA, M. PIJOLAT and R. LALAUZE, *J. Mater. Sci.* **23** (1988) 2960.
66. M. PIJOLAT, V. CHIAVAZZA and R. LALAUZE, *Appl. Surf. Sci.* **31** (1988) 179.
67. J. C. EHRSTROM, E. ANDRIEU and A. PINEAU, *Scripta Metall.* **23** (1989) 1397.
68. J. L. ESTRADA and J. DUSZCZYK, *J. Mater. Sci.* **25** (1990) 886.
69. J. L. ESTRADA and J. DUSZCZYK, *ibid.* **25** (1990) 1381.
70. A. LAWLEY, *Ann. Rev. Mater. Sci.* **8** (1978) 49.
71. *Idem, J. Metals* **33** (January 1981) 13.
72. A. LAWLEY and R. D. DOHERTY, in "Proceedings on Rapidly Solidified Crystalline Alloys", Morristown, May 1985, edited by S. K. Das, B. H. Kear and C. M. Adam (The Metallurgical Society of AIME, Warrendale, Pennsylvania, 1985) p. 77.
73. N. J. GRANT, in "Industrial Materials Science and Engineering", edited by L E. Murr (Marcel Dekker, New York and Basel, 1984) p. 251.
74. R. M. GERMAN, Powder Metallurgy Science (Metal Powder Industries Federation, Princeton, New Jersey, 1984) p. 75.
75. J. B. SEE and G. H. JOHNSTON, *Powder Metall.* **21** (1978) 119.
76. N. DOMBROWSKI and W. R. JOHNS, *Chem. Engng. Sci.* **18** (1963) 203.
77. J. DUSZCZYK, J. L. ESTRADA, L. BUEKENHOUT and R. YOSHIMURA, in "Proceedings of International Conference on Hot Isostatic Pressing of Materials: Applications and Developments", Antwerp, April 1988 (The Royal Flemish Society of Engineers, Antwerp, 1088) p. 265.
78. C. E. RANSLEY and H. NEUFELD, *J. Inst. Metals* **74** (1948) 599.
79. C. E. RANSLEY, D. E. TALBOT and H. C. BARLOW, *ibid.* **86** (1957–58) 212.
80. K. J. BRONDYKE and P. D. HESS, *Trans. Met. Soc. AIME* **230** (1964) 1542.
81. P. D. HESS, *J. Metals* **25** (October 1973) 46.
82. K. ALKER, *Giesserei* **61** (23) (1974) 693.
83. A. CHOUDHURY and M. LORKE, *Aluminium* **65** (5) (1989) 462.
84. H. BREGGEMAN, *Gietwerk Perspektief*, **6** (5) (September/October 1986) 30.
85. W. EICHENAUER, K. HATTENBACH and A. PEBLER, *Z. Metallkde* **52** (1961) 682.
86. W. R. OPIE and N. J. GRANT, *Trans. AIME* **188** (1950) 12137.
87. E. FROMM and E. GEBHARDT, "Gase und Kohlenstoff in Metallen" (Springer-Verlag, Berlin, 1976).
88. H. JEHN, *ibid.* p. 268.
89. G. HÖRZ, *ibid.* p. 84.
90. K. WEFERS and Ch. MISRA, in "Oxides and Hydroxides of Aluminium", Alcoa Technical Paper no. 19, Alcoa Laboratories, pp. 36, 47.
91. L. K. HUDSON, in "Production of Aluminium and Alumina" (Wiley, Chichester, 1987) p. 32.
92. M. VOGEL, in "Nichtmetalle in Metallen", Münster, 1986, edited by D. Hirschfeld (Deutsche Gesellschaft für Metallkunde, Oberursel, 1987) p. 197.
93. J. L. ESTRADA and J. DUSZCZYK, unpublished research, Delft University of Technology.
94. J. DUSZCZYK, J. L. ESTRADA, B. M. KOREVAAR, Z. FANG, T. L. J. de HAAN and P. COLIJN, Technical Report for Showa Denko K.K., October 1987 (Japan), Delft University of Technology, the Netherlands.
95. I. BARIN and O. KNACKE, Thermochemical properties of inorganic substances (Springer-Verlag, Berlin, 1973) pp. 11, 32, 34, 35, 316, 323, 433, 441, 584.
96. O. KUBASCHEWSKI and C. B. ALCOCK, Metallurgical Thermochemistry, 5th Edn (Pergamon Press, London, 1979) p. 3.
97. J. J. MOORE, E. A. BOYCE, M. J. BROOKS, B. PERRY and P. J. SHERIDAN, Chemical Metallurgy (Butterworths, London, Boston, 1981) p. 69.
98. T. S. LUNDY and J. F. MURDOCK, *J. Appl. Phys.* **33** (1962) 1671.

Received 24 November 1989
and accepted 19 February 1990